RSC Advances

ROYAL SOCIETY OF CHEMISTRY

www.rsc.org/advances

Ultrasonic preparation of tungsten disulfide single-layers and quantum dots

Václav Štengl*, Jakub Tolasz, Daniela Popelková

Department of Material Chemistry, Institute of Inorganic Chemistry AS CR v.v.i.,

250 68 Řež, Czech Republic

E-mail:stengl@iic.cas.cz

Abstract: Natural raw mineral tungstenite (WS_2) was exfoliated to single-layer sheets using high intensity ultrasound. Exfoliation of bulk layered materials, such as WS_2 by ultrasound is an attractive way to a large-scale preparation of mono- or few-layered crystals. To evaluate a quality of delamination X-ray diffraction, Raman spectroscopy and microscopic techniques (TEM and AFM) were employed. The obtained exfoliated product served as precursor for quantum dots preparation using simple refluxing in ethylene glycol. The synthesized WS_2 quantum dots were characterized by photoluminescence spectroscopy and AFM microscopy. Exfoliated WS_2 thus can join the group of similarly prepared single-layers of MoS_2 or graphene.

Keywords: tungstenite, single layer sheets, ultrasound, quantum dots

1.Introduction

Two-dimensional materials and minerals are nowadays of major interest for many research groups around the world. In the recent years major interest paid to graphene due to its unique physical and chemical properties. However, attention pay also to other layered materials, so called inorganic analogues of graphene (IAG), despite the obstacles in simple preparation of mono- or few-layer flakes of these materials in sufficient quality, purity and quantity. Wide range of these materials have huge potential both for basic research and applications.

IAG include transition metal dichalcogenides (MoS_2, WS_2, TaS_2), transition metal oxides (ZnO, MoO_6, V_2O_5) and nitrides (h-BN, h-BCN, g-C_3N_4). Among natural minerals graphite-like layered structure possess chalkogenides of Mo and W - molybdenite (MoS_2), tungstenite (WS_2), and drysdallite $(MoSe,S)_2$.

To fairly new findings on the preparation of monolayered IAGs belongs exfoliation of WS_2 by ultrasonic treatment by n□butylithium in hexane which was found more difficult than the exfoliation of MoS_2 [1], [2]. The difficulty was found to be the resistance of the WS_2 to intercalation [3], [4]. Single layers of the transition-metal dichalcogenides WS_2, MoS_2, and $MoSe_2$ were formed as aqueous suspensions by lithium intercalation and exfoliation of crystalline powders [5]. Rao at al. [6], [7] described preparation of WS_2 and MoS_2 using intercalation with lithium followed by exfoliation of the layers by ultrasonication and chemical synthesis, where molybdic and tungstic acid respectively, was treated with excess of thiourea. Guardia at al. [8] demonstrated several non-ionic surfactants to be very efficient stabilizers for the production of stable aqueous dispersions of MoS_2 and WS_2 platelets partially exfoliated by sonication. Gelatin was used for exfoliation of graphene, MoS_2, WS_2 and BN at the low concentration of 0.6-1.4 mg/mL [9].

Surface functionalised WS_2 nanosheets were prepared by a strong acid treatment with chlorosulfonic acid HSO_3Cl, followed by quenching in deionized water [10]. The methods to separate layered materials such as ion intercalation, in which metal ions are inserted between layers and a charge is transferred to the layers causing them to repel each other, can change the chemical structure of the layers, are time consuming and need to be carried out under an inert atmosphere. A

mixed-solvent strategy, low intensity treatment of ultrasound (ultrasonic bath), was used for exfoliation of MoS_2, WS_2 and BN in the ethanol/water mixtures [11]. This method provide only suspension with around 1% exfoliated particles. Coleman et al. [12] used common solvents such as n-methyl pyrrolidone to exfoliate (separate) layered materials such as boron nitride BN, molybdenum disulfide MoS_2, tungsten disulfide WS_2 and bismuth telluride Bi_2Te_3 into individual sheets.

Gutiérrez at al. [13] presented the direct synthesis of WS_2 monolayers with triangular morphologies and strong room-temperature photoluminescence. Bulk WS_2 did not present PL due to its indirect band gap nature. The edges of these monolayers exhibited PL signals with extraordinary intensity, around 25 times stronger than the platelets centre. Graphene-like and plate-like WS_2 were prepared by solid-state reaction of powder sulphur and tungsten at 500°C [14]. Thin films of WS_2 were grown by metal-organic van der Waals-epitaxy using $W(CO)_6$ and Sn as precursors, which lead to high quality films on the expense of a very inefficient deposition. A single and few layers of BN, MoS_2 and WS_2 were obtained via direct exfoliation of powder materials using supercritical CO_2 assisted with ultrasound. The effects of supercritical CO_2 coupled with ultrasound play a key role in the exfoliation process [15]. Gan at al [16] refer about physical properties of two-dimensional quantum dots MoS2 and He at al [17] about WS2. Hydrophobous MoS2 / WS2 quantum dots in dimethylformamide were prepared [18].

In this paper we present method of preparation monolayers from natural mineral tungstenite WS_2 by effect of stationary ultrasound waves in pressurised reactor. This method is based on the experience in the preparation of MoS_2 quantum dots from mineral molybdenite [19]. Exfoliation using power ultrasound allows preparation of nanosheets suspension with versatile applications. The exfoliated monolayered WS_2 was then used for simple synthesis of WS_2 quantum dots (WSQDs).

2. Experimental

Ethylene glycol (EG) were supplied by Sigma–Aldrich Ltd., the natural minerals tungstenite WS_2 from US Research Nanomaterials Inc.

2.1. Preparation of exfoliated WS_2

Delaminated WS_2 was prepared from natural tungstenite by using a high-intensity cavitation field in a pressurized ultrasound reactor (UIP2000 hd, 20 kHz, 2000 W, Hielscher Ultrasonics, GmbH). Natural tungstenite (0.5 g) was suspended in 120 ml of EG and exposed to high intensive ultrasound for 20 min (samples denoted as WS_2 exfoliated). The pressure of 6 bar was set in the reactor by means of an air compressor [20]. The exfoliated sample WS_2 was purged from EG solution by dialysis using Spectra/Por® Membrane. The final product was filtered off using a Pragopor membrane filter, washed with ethanol and dried at 105 °C.

2.2. Preparation of WS_2-quantum dots

The WSQDs were easily prepared by refluxing exfoliated WS_2 (0.1 g) nanosheets obtained by sonication in EG (100 ml) at atmospheric pressure for 96 hours. The resulting dispersion was filtered off using a Pragopor membrane filter and a clear transparent solution was obtained. The schematic of exfoliation WS2 using high intensity ultrasound and next ethylene glycol reflux illustrated Figure 1.

2.3. Characterization methods

Diffraction patterns were collected using a PANalytical X´Pert PRO diffractometer equipped with a conventional X-ray tube (CuKα 40 kV, 30 mA, line focus) in a transmission mode. An elliptic focusing mirror, a divergence slit 0.5°, an anti-scatter slit 0.5° and a Soller slit of 0.02 rad were used in the primary beam. A fast linear position sensitive detector PIXcel with an anti-scatter shield and a Soller slit of 0.02 rad were used in the diffracted beam. All patterns were collected in the range of 1 to 85 deg. 2theta with the step of 0.013 deg and 500 sec/step. A qualitative analysis was performed with the DiffracPlus Eva software package (Bruker AXS, Germany) using the JCPDS

PDF-2 database [21]. A water suspension of sample was placed onto a sample holder for transmission experiments covered with a mylar foil (6 μm thick). Then, the second mylar foil covered the sample to avoid losses. Finally, the sample holder was fixed with a sample holder ring and thus was sample ready for measurement in a transmission mode. The crystallite size, interlayer spacing and number of WS_2 layers were calculated by using the classical Debye–Scherrer equation [22], [23].

The morphology of the tungstenite samples was inspected by transmission electron microscopy (TEM) using a 300 kV TEM microscope JEOL 3010F. As a specimen support for TEM investigations, a microscopic copper grid covered by a thin transparent carbon film was used.

High resolution transmission electron microscope (HRTEM) analysis was performed on FEI Talos F200X. The microscope is equipped with Super-X EDS system with four silicon drift detectors (SDDs) for precise and quantitative energy dispersive X-ray (EDS) analysis for advanced materials characterization. The 300 Mesh Regular Copper Grid coated by Silicon Dioxide (SiO_2) / Monoxide (SiO) were used for sample preparation.

AFM images were obtained using a Bruker Dimension FastScan microscope. The sample was prepared by pipetting the exfoliated WS_2 water suspension onto a synthetic mica (an atomically smooth support), the sample was then spin coated at 6000 RPM for one minute. For measurement was used silicon tip on nitride lever with ScanAsyst - air contact mode in resonance frequencies ranging from 50 to 90 kHz. Particle size distribution was done by programme Nanoscope Analysis (Bruker, USA).

The Raman spectra were acquired with a DXR Raman microscope (Thermo Scientific) using a 532 nm (0.3 mW) laser; 1024 two-second scans were accumulated with the laser using the 10x objective of an Olympus microscope.

The luminescence properties of the quantum dots were determined by Avantes AvaSpec 2048 equipped with high power (5W) LEDs at wavelengths 365, 375, 385, 400 and 405 nm as an excitation sources.

3. Results and discussion

As well as graphene, IAG must be exfoliated preferably to monolayers to exploit their full potential. Transition metal dichalcogenides can be exfoliated by ion intercalation. This method is environment friendly, but time consuming and it is not suitable for most applications. Intercalation of MoS_2 by buthylithium results in loss of the semiconducting properties due to emergence of a metallic phase [11]. Subsequent removal of the intercalation ions leads to a reaggregation of layers. Hernandez et al. [24] used method of liquid-phase exfoliation, where the surface energy of the solvent is advantageously used to exfoliate the graphite. Surface energy of graphene, which is about 70 mJ/m^2 is in the upper range of surface energies for most solvents. Therefore this method can not be used for exfoliation IAG, because the surface energies of these materials have been determined to be considerably higher than that of graphene. For example Weiss et al. [25] referred, that surface energies of transition metal dichalcogenides such as MoS_2 and WS_2 are greater than 200 mJ/m^2. Since there are no suitable solvents, the method of liquid-phase exfoliation can not be used for exfoliation of IAGs.

Recently we have shown, that graphite [20] can be exfoliated by high intensity ultrasound in strong polar aprotic solvents. This method was then successfully used for MoS_2 delamination [19] and in here we applied this method to WS_2. Figure 2 presented the XRD spectrum of raw and exfoliated WS_2 tungstenite corresponding to the PDF card 08-0237. As can be seen, the exfoliated WS_2 deposited as transparent layer on silicon holder have dominant diffraction line at $2\theta = 14.3°$. Inset shows diffraction pattern of the exfoliated WS_2 sample recorded in a water suspension between two Mylar follies in order to avoid drying and re-stacking of layers. The crystallite size was calculated to be 7.57 nm for the (002) plane, which is in accordance with results of synthetic WS_2 [14].

The Raman spectrum of exfoliated WS_2 is presented in Figure 3. The Raman active modes in WS_2 were found at positions 42 cm^{-1} (E^2_{2g}), 317 cm^{-1} (E_{1g}), 346 cm^{-1} (E^1_{2g}) and 415 cm^{-1} (A_{1g}) [26]. Decreasing of the number of layers caused blue-shift of the E^2_{2g} mode, which is consistent with previous reports [14, 27]. Inset presents blue-shift of E^2_{2g} mode in dependence on time of ultrasound irradiation. The similar behavior was observed for MoS_2 [19]. In general, the WS_2 phonon bands are

shifted down to lower frequencies with respect to the MoS_2 which may be caused by the larger mass of the tungsten atoms [28]. No shift or broadening was observed for the A_{1g} mode due to structural disordering [27].

Raw and exfoliated sample of WS_2 were investigated by TEM (Figure 4). The layered structure of bulk material is clearly visible (Figure 4a). After sonication are the layers effectively exfoliated and final product contains flakes of monolayers (Figures 4b). HRTEM investigations (see Fig4.c-d) revealed the hexagonal lattice structure with the lattice spacing of 0.315 nm, 0.317 nm and 0.318 nm assigned to the (100) plane (d = 0.309 nm [004], PDF 84_1398). Further, HRTEM results indicate that the inner part of the nanosheets has a well-crystallographic structure without existence of defects. The flakes are smooth, several μm large, without any visible defects. We emphasize the product is not contaminated, since no intercalation or other chemicals (except the solvent - EG) were used.

According to Miller–Bravais indices (hkl) of exfoliated WS_2 sample, each set of diffraction spots exhibited an inner hexagon that corresponded to (1-110) indices and an outer hexagon that corresponded to (1-210) indices. The intensity profiles of the WS_2 diffraction patterns could be used to determine the number of layers in the WS_2 sheet. The relative intensities of the diffraction spots in the inner and outer hexagons were shown to be equivalent in single-layer WS_2. Bi-layers has relative intensities of the spots in the outer hexagon twice of those in the inner hexagon [29]. The SAED of prepared exfoliated sample (Figure 5) showed the typical six-fold symmetry that is expected for graphite-like WS_2. The intensity of a line section through the (1-210), (0-110), (-1010), and (-2110) spots is shown in the inset. The inner (0-110)- and (-1010)-type reflections are more intense than the outer (1-210)- and (-2110)-type reflections which is consistent with isolated single-layer.

Figure 6 shows the typical tapping-mode AFM image of exfoliated WS_2 deposited on a mica substrate. According to cross-sectional analysis the exfoliated sheet of WS_2 posses thickness lower

than < 0.8 nm, which correspond to single-layer [30]. This result support the HRTEM observation, that exfoliated monolayers of WS_2 were obtained. Lateral sheet size is < 800 x 900 nm.

Refluxing the exfoliated product in EG for 96 hour provides strongly blue luminescent dispersion under UV excitation light, observable by naked eye (see Figure 7). High resolution electron microscopy (HRTM) of these solution showed in Figure 8 uniform quantum dots in size < 2 nm. The interlayer spacing (d-spacing) were calculated to < 0.27 nm, which corresponds to (100) plane of WS2 (PDF card 08-0237). Mapping of elements of the same solution sample, where atoms of W are displayed red and atoms of S are displayed green is presented in Figure 9.

AFM analysis revealed small dots of few nm size present in the sample after refluxing (Figure 10). These quantum dots could be then stabilized, since the proper solvent (EG) encapsulate the particles and prevent them to agglomerate [31]. The particle size analysis showed that the particles are up to < 2 nm thick, but most of them are around only < 1 nm.

The luminescence properties of the prepared quantum dots dispersions were investigated at different excitation wavelengths from 365 to 405 nm (Figure 11). Increasing wavelength of the excitation light, lead to shift of the emission maxima of the dispersion. The excitation-dependent luminescence indicates polydispersity of the prepared WS_2 quantum dots, which is characteristic for our method of synthesis.

The use of ultrasound is a simple and effective method for preparing exfoliated materials. This method allow to isolate nano-dimensional inorganic layers of other layered compounds. The exfoliated layers may serve as building blocks for new nano-layered composite materials prepared by the layer-by-layer method. Ease of the ultrasonic exfoliation allow effectively increase the yield of the production and may put these attractive materials to practice.

Conclusions

The exfoliated WS_2 few- and single-lyers were prepared from natural tungstenite by using high intensity ultrasound in a pressurized ultrasonic batch reactor. Ultrasound can transfer high energy into matter and weaken the Van der Waals forces between adjacent layers, which result in effective delamination. Increasing the pressure in the reactor loads the end of ultrasound horn and consequently lead to higher energy transfer (to the power 2000 watts) into the reaction solution. The conditions in the ultrasonic reactor such as pressure, temperature, ultrasound power, and processing time tune the process of exfoliation. Stationary ultrasound waves were successfully used beside here reported WS_2 for exfoliation of other layered minerals such as graphite or molybdenite, and synthetic materials like BN and BCN. The ease of single layered quantum dots preparation also proves the quality of process of ultrasound exfoliation itself. Delamination of WS_2 was found to be more difficult than the MoS_2, as previously reported. The effective delamination was achieved after nearly twice longer time in the reactor than in case of MoS_2.

Acknowledgement: This work was supported by Grant Agency of the Czech Republic (project 14-05146S).

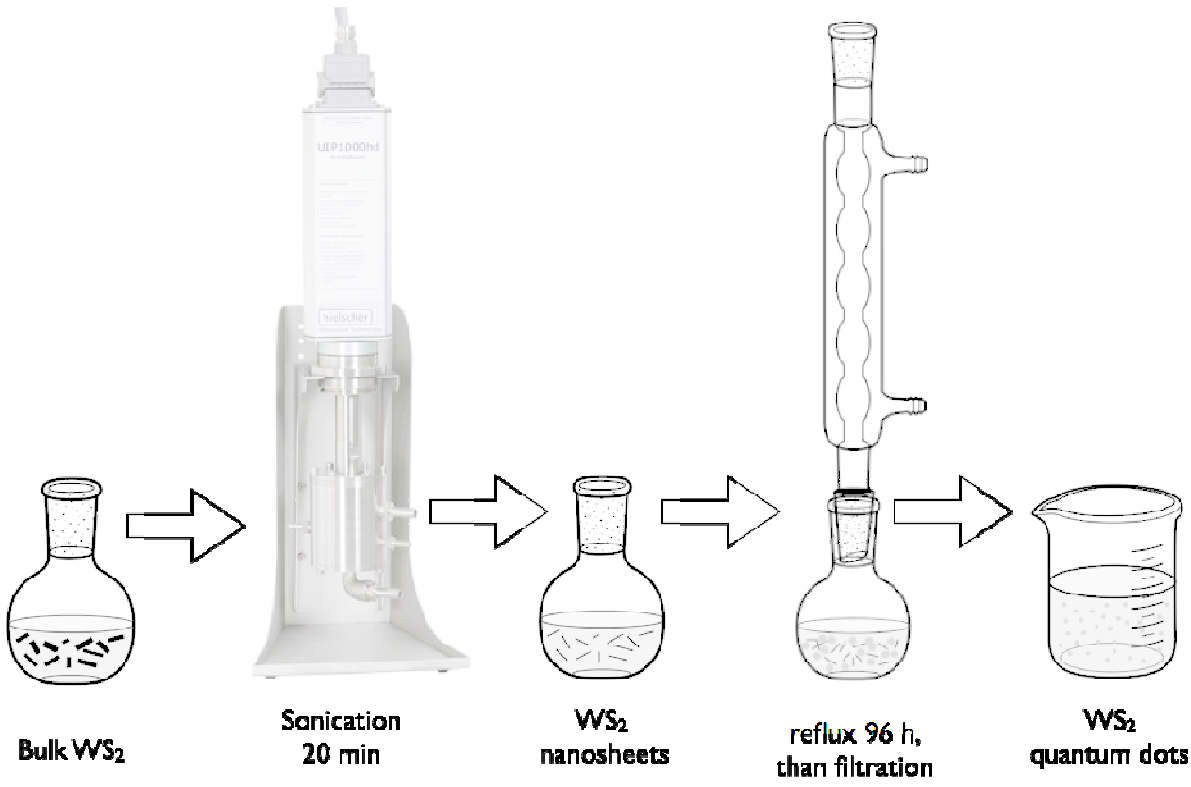

Figure 1. Schematic of exfoliation bulk WS2 and quantum dots preparation using reflux

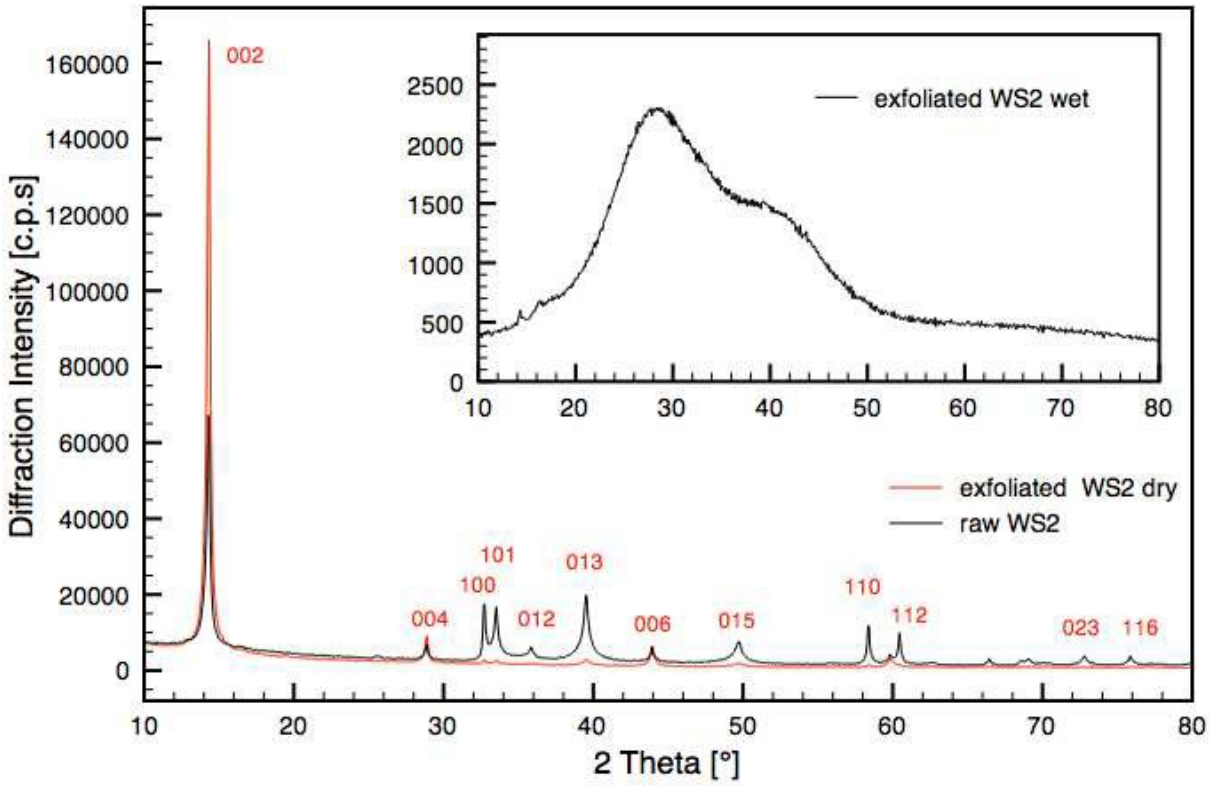

Figure 2. XRD pattern of bulk WS_2 and exfoliated sample

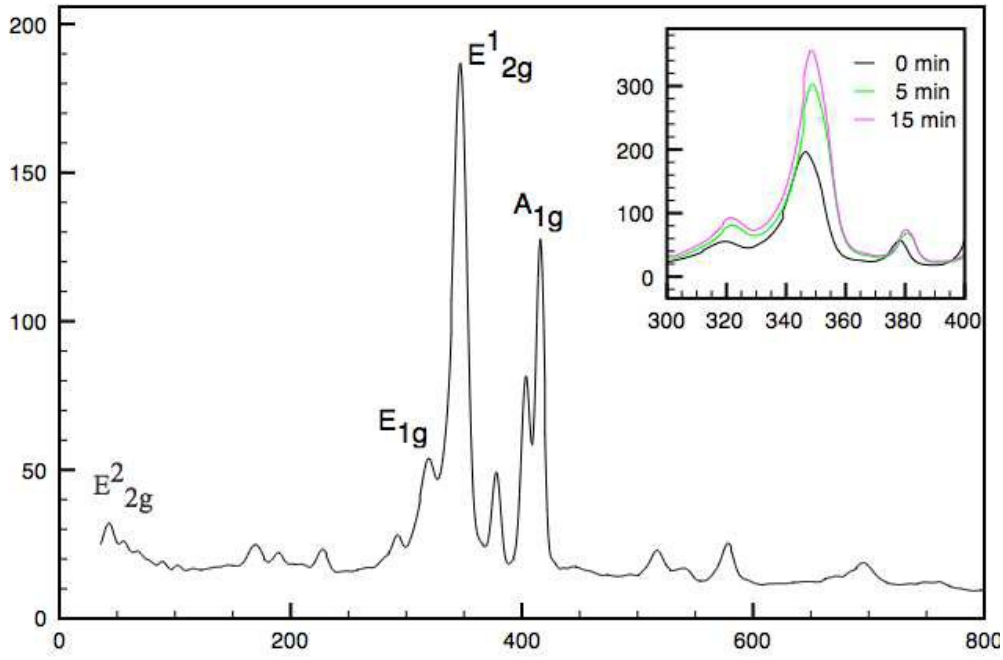

Figure 3. Raman spectrum of bulk WS_2. Inset exfoliated samples

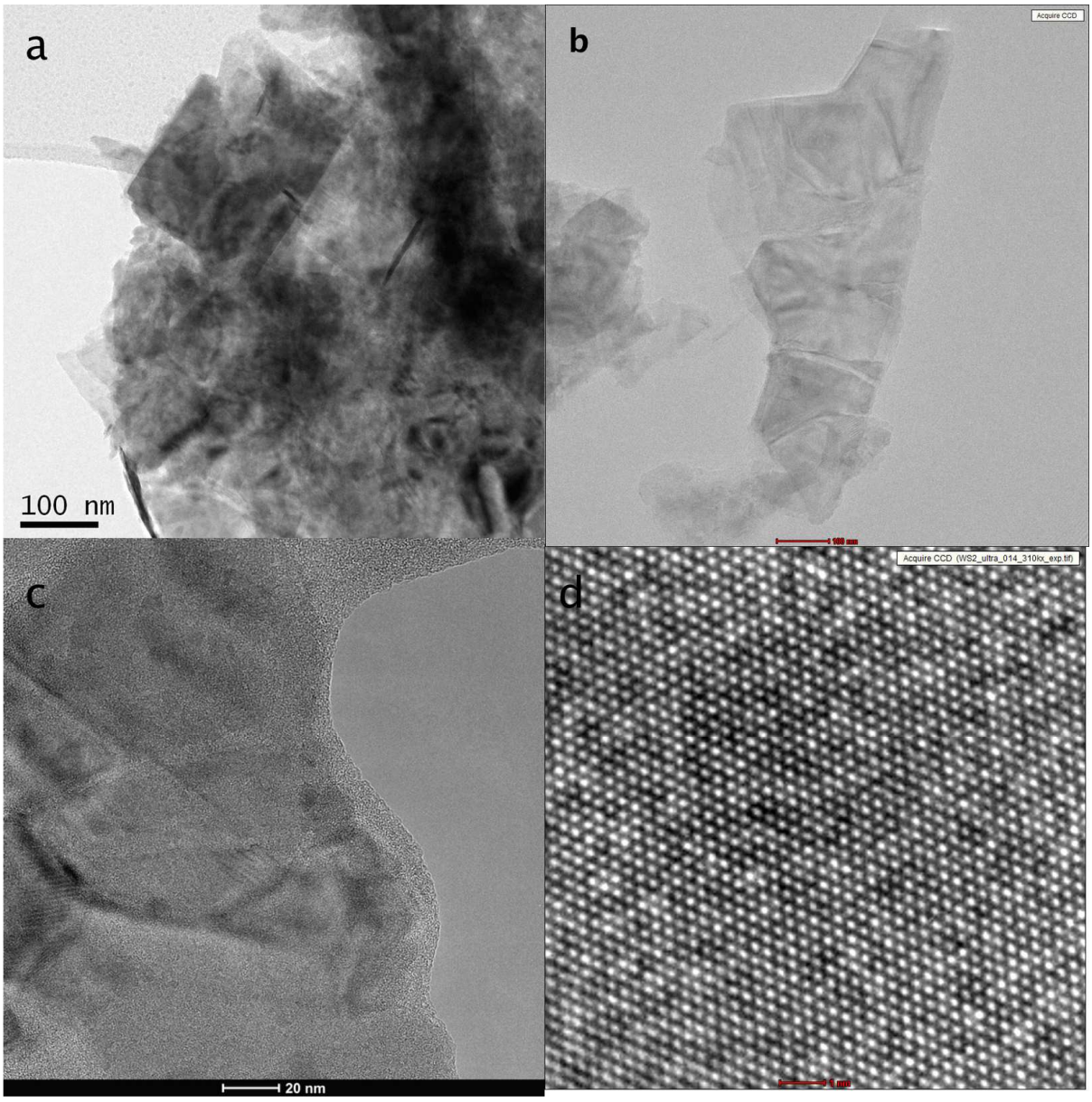

Figure 4. TEM images of a) raw WS_2, HRTEM images of ultrasound exfoliated sample b) magnification 450 000y c) magnification 310 000x and d) magnification 4 115 000x

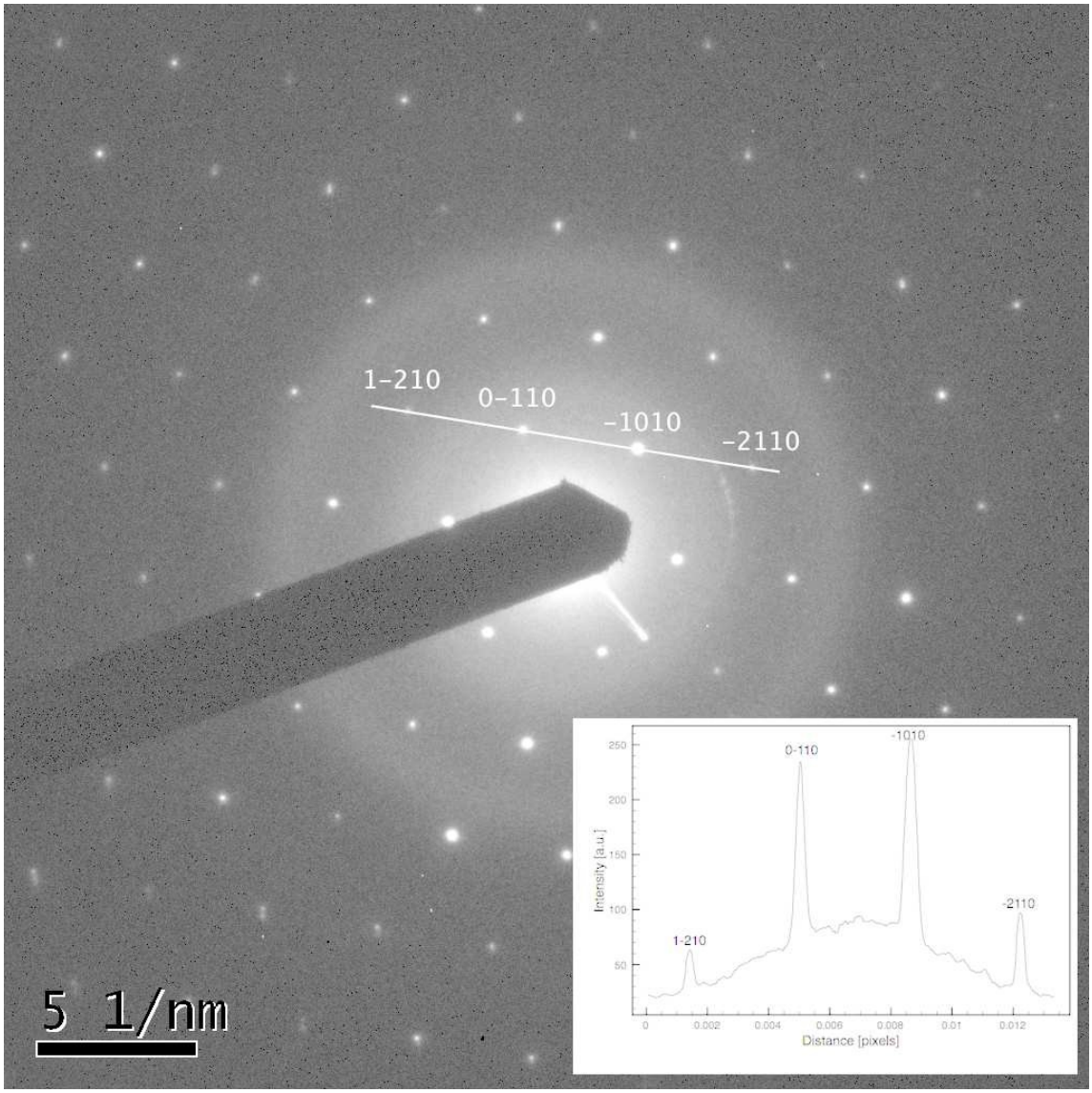

Figure 5. Selected Area Electron diffraction (SAED) of exfoliated WS_2 sample. Inset intensity of a line section through the (1-210), (0-110), (-1010), and (-2110) spots

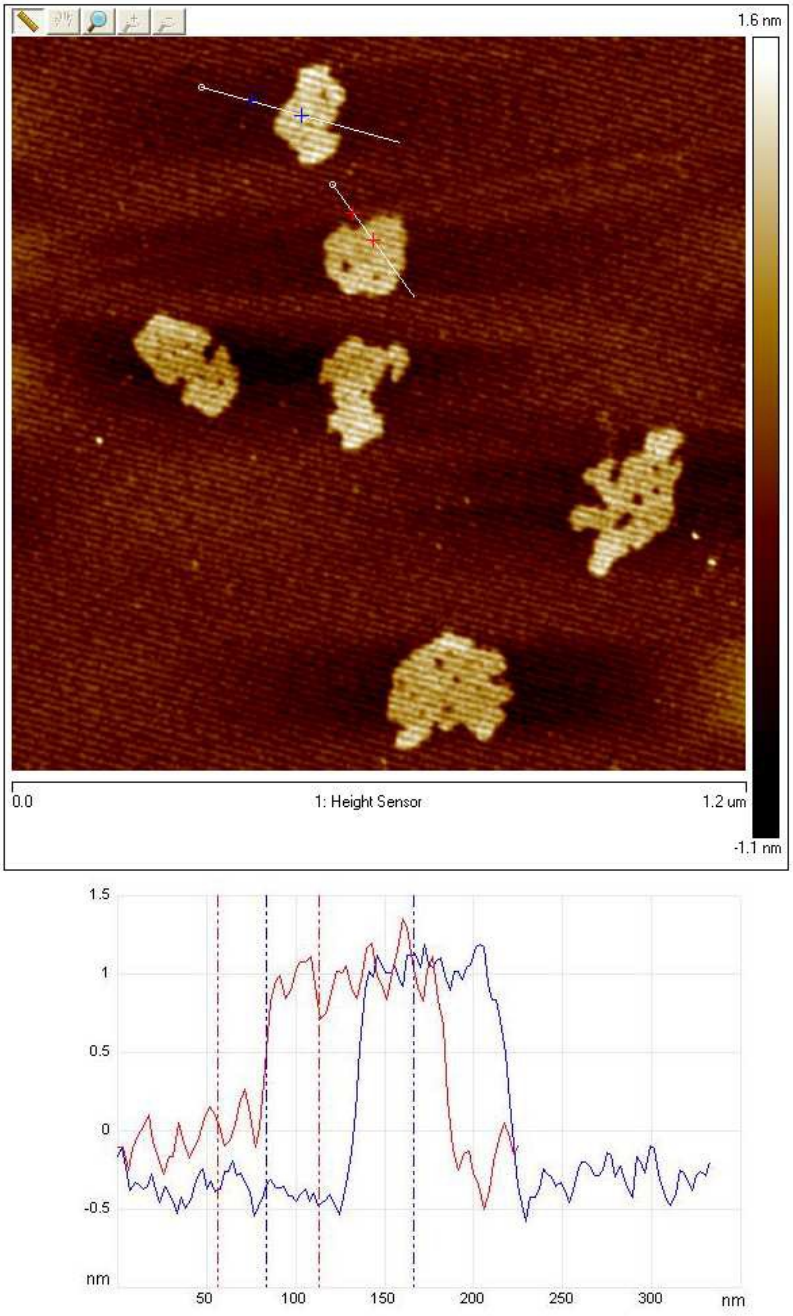

Figure 6. AFM images of exfoliated tungstenite WS_2

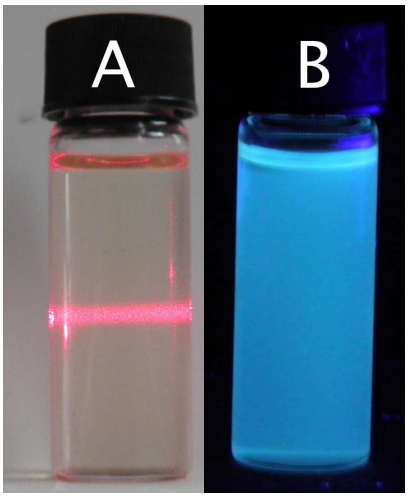

Figure 7. Photograph of luminescent WS_2 quantum dots under A) daylight and b) UV light (365 nm)

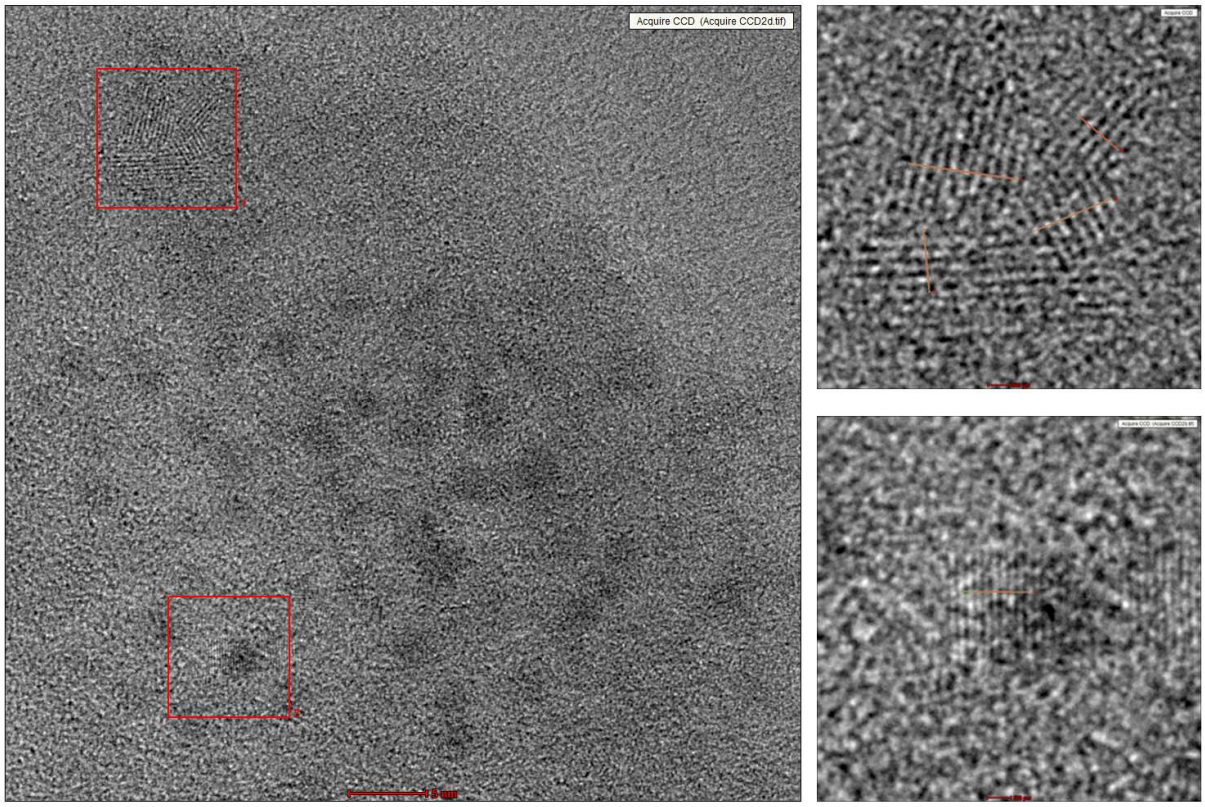

Figure 8. HRTEM images of solution exfoliated WS2 after ethylene glycol reflux

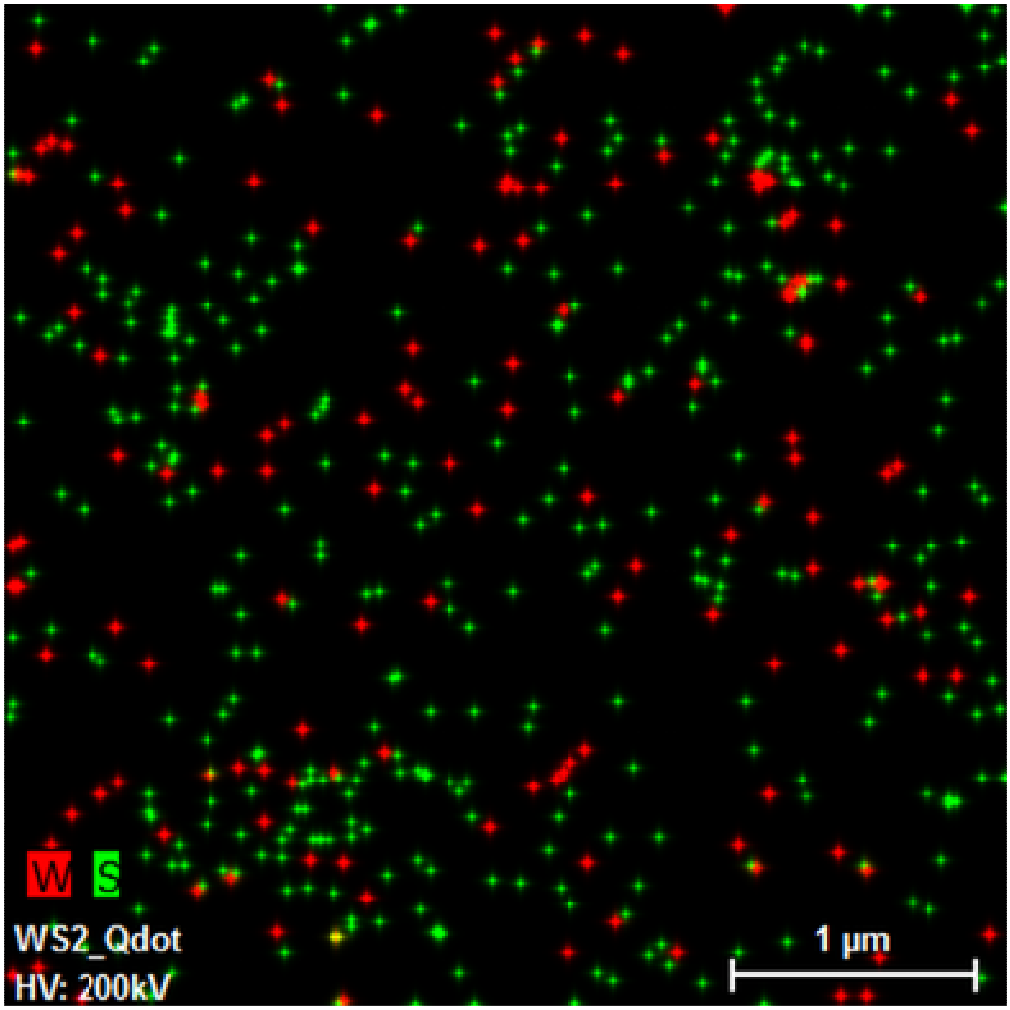

Figure 9. Mapping of elements W (red) and S (green) of solution exfoliated WS2 after ethylene glycol reflux

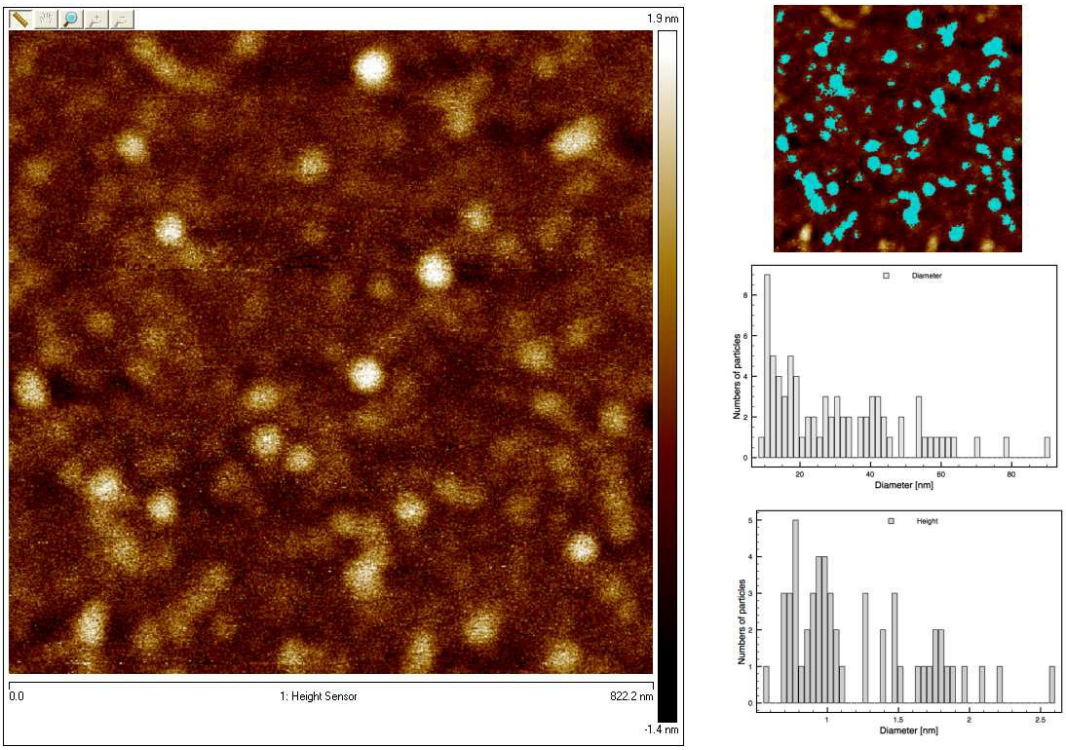

Figure 10. AFM images of WS_2 quantum dots and particle size analysis - number of particles versus diameter and height.

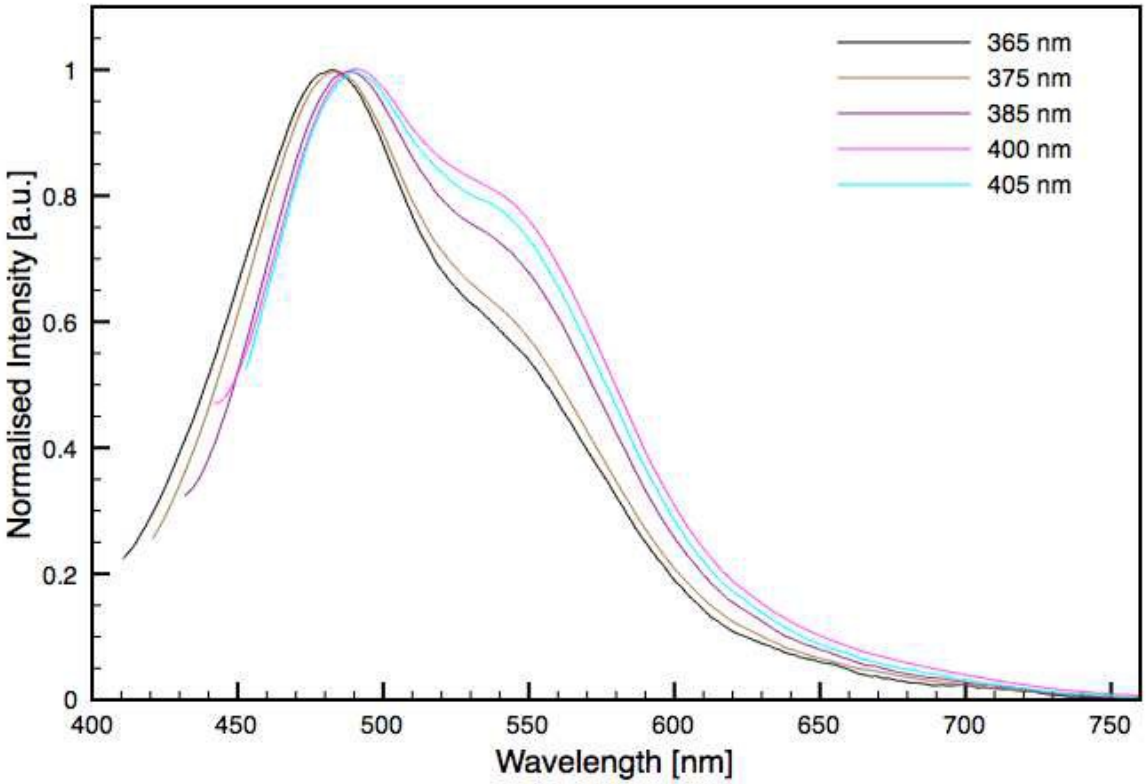

Figure 11. Normalised excitation luminescence spectra of WS_2 quantum dots

References:

1.B. K. Miremadi, T. Cowan and S. R. Morrison, *Journal of Applied Physics*, 1991, **69**, 6373-6379.
2.B. K. Miremadi and S. R. Morrison, *Surface Science*, 1986, **173**, 605-617.
3.B. K. Miremadi and S. R. Morrison, *Journal of Applied Physics*, 1988, **63**, 4970-4974.
4.D. Yang and R. F. Frindt, *Journal of Physics and Chemistry of Solids*, 1996, **57**, 1113-1116.
5.R. A. Gordon, D. Yang, E. D. Crozier, D. T. Jiang and R. F. Frindt, *Physical Review B*, 2002, **65**.
6.C. N. R. Rao and A. Nag, *European Journal of Inorganic Chemistry*, 2010, DOI: 10.1002/ejic.201000408, 4244-4250.
7.C. N. R. Rao, H. S. S. R. Matte and U. Maitra, *Angewandte Chemie-International Edition*, 2013, **52**, 13162-13185.
8.L. Guardia, J. I. Paredes, R. Rozada, S. Villar-Rodil, A. Martinez-Alonso and J. M. D. Tascon, *Rsc Advances*, 2014, **4**, 14115-14127.
9.Y. Ge, J. Wang, Z. Shi and J. Yin, *Journal of Materials Chemistry*, 2012, **22**, 17619-17624.
10.R. Bhandavat, L. David and G. Singh, *Journal of Physical Chemistry Letters*, 2012, **3**, 1523-1530.
11.K.-G. Zhou, N.-N. Mao, H.-X. Wang, Y. Peng and H.-L. Zhang, *Angewandte Chemie-International Edition*, 2011, **50**, 10839-10842.
12.J. N. Coleman, M. Lotya, A. O'Neill, S. D. Bergin, P. J. King, U. Khan, K. Young, A. Gaucher, S. De, R. J. Smith, I. V. Shvets, S. K. Arora, G. Stanton, H.-Y. Kim, K. Lee, G. T. Kim, G. S. Duesberg, T. Hallam, J. J. Boland, J. J. Wang, J. F. Donegan, J. C. Grunlan, G. Moriarty, A. Shmeliov, R. J. Nicholls, J. M. Perkins, E. M. Grieveson, K. Theuwissen, D. W. McComb, P. D. Nellist and V. Nicolosi, *Science*, 2011, **331**, 568-571.
13.H. R. Gutierrez, N. Perea-Lopez, A. L. Elias, A. Berkdemir, B. Wang, R. Lv, F. Lopez-Urias, V. H. Crespi, H. Terrones and M. Terrones, *Nano Letters*, 2013, **13**, 3447-3454.
14.X. Fang, C. Hua, C. Wu, X. Wang, L. Shen, Q. Kong, J. Wang, Y. Hu, Z. Wang and L. Chen, *Chemistry-a European Journal*, 2013, **19**, 5694-5700.

15.Y. Wang, C. Zhou, W. Wang and Y. Zhao, *Industrial & Engineering Chemistry Research*, 2013, **52**, 4379-4382.
16.Z. X. Gan, L. Z. Liu, H. Y. Wu, Y. L. Hao, Y. Shan, X. L. Wu and P. K. Chu, *Applied Physics Letters*, 2015, **106**, 233113.
17.Y.-M. He, G. Clark, J. R. Schaibley, Y. He, M.-C. Chen, Y.-J. Wei, X. Ding, Q. Zhang, W. Yao, X. Xu, C.-Y. Lu and J.-W. Pan, *Nature Nanotechnology*, 2015, **10**, 497-502.
18.S. Xu, D. Li and P. Wu, *Advanced Functional Materials*, 2015, **25**, 1127-1136.
19.V. Stengl and J. Henych, *Nanoscale*, 2013, **5**, 3387-3394.
20.V. Stengl, *Chemistry-a European Journal*, 2012, **18**, 14047-14054.
21. JCPDS, 2000.
22.B. Sakintuna, S. Cetinkaya and Y. Yurum, *Energy & Fuels*, 2004, **18**, 883-888.
23.B. Saner, F. Okyay and Y. Yurum, *Fuel*, 2010, **89**, 1903-1910.
24.Y. Hernandez, V. Nicolosi, M. Lotya, F. M. Blighe, Z. Sun, S. De, I. T. McGovern, B. Holland, M. Byrne, Y. K. Gun'ko, J. J. Boland, P. Niraj, G. Duesberg, S. Krishnamurthy, R. Goodhue, J. Hutchison, V. Scardaci, A. C. Ferrari and J. N. Coleman, *Nature Nanotechnology*, 2008, **3**, 563-568.
25.K. Weiss and J. M. Phillips, *Physical Review B*, 1976, **14**, 5392-5395.
26.M. Virsek, A. Jesih, I. Milosevic, M. Damnjanovic and M. Remskar, *Surface Science*, 2007, **601**, 2868-2872.
27.C. Lee, H. Yan, L. E. Brus, T. F. Heinz, J. Hone and S. Ryu, *Acs Nano*, 2010, **4**, 2695-2700.
28.A. Molina-Sanchez and L. Wirtz, *Physical Review B*, 2011, **84**.
29.A. Dato, V. Radmilovic, Z. Lee, J. Phillips and M. Frenklach, *Nano Letters*, 2008, **8**, 2012-2016.
30.P. Tonndorf, R. Schmidt, P. Boettger, X. Zhang, J. Boerner, A. Liebig, M. Albrecht, C. Kloc, O. Gordan, D. R. T. Zahn, S. M. de Vasconcellos and R. Bratschitsch, *Optics Express*, 2013, **21**, 4908-4916.
31.H. Li, Z. Kang, Y. Liu and S.-T. Lee, *Journal of Materials Chemistry*, 2012, **22**, 24230-24253.